Available online at www.sciencedirect.com
ScienceDirect
Ceramics International 37 (2011) 3575–3581
CERAMICS INTERNATIONAL
www.elsevier.com/locate/ceramint

Solubility limits and microwave dielectric properties of $Ba_{6-3x}Sm_{8+2x}Ti_{18}O_{54}$ solid solution

Li Zhong, Xiao Li Zhu, Xiang Ming Chen *, Xiao Qiang Liu, Lei Li

Laboratory of Dielectric Materials, Department of Materials Science and Engineering, Zhejiang University, Hangzhou 310029, China

Received 13 April 2011; received in revised form 8 June 2011; accepted 8 June 2011
Available online 14 June 2011

Abstract

Upper and lower solubility limits in $Ba_{6-3x}Sm_{8+2x}Ti_{18}O_{54}$ tungsten bronze ceramics were determined by Rietveld refinement of XRD data combined with backscattered electron images, and the variation tendency of microwave dielectric characteristics was also investigated. The upper solubility limit was confirmed as $x = 2/3$, while the lower solubility limit was determined as 1/4 instead of the previously reported one $x = 3/10$. The dielectric constant of $Ba_{6-3x}Sm_{8+2x}Ti_{18}O_{54}$ ceramics decreases monotonically with increasing x, while the small temperature coefficient of resonant frequency with complex variation tendency is observed for the compositions $1/2 \leq x \leq 4/5$. The Qf value increases at first, reaches the maximum around $x = 2/3$, and turns to decrease for $x > 7/10$.

Keywords: Rietveld refinement; Microwave dielectric properties; Solubility limits

1. Introduction

Microwave dielectric ceramics have been intensively studied over decades because of their important applications as resonators, filters, and other key components in microwave communication systems [1]. The development of microwave telecommunication technology has been significantly promoted by the microwave dielectric ceramics exhibiting high permittivity (ε_r), low dielectric loss (tan δ) and near-zero temperature coefficient of resonant frequency (τ_f). Many systems have been investigated for developing new materials, but only a limited number lead to interesting characteristics. Among them, the tungsten bronze type $Ba_{6-3x}R_{8+2x}Ti_{18}O_{54}$ (R: rear earth) solid solutions have attracted much scientific and commercial interests as the most important high-ε microwave dielectric materials [2–20].

The $BaO–R_2O_3–TiO_2$ system was first investigated by Bolton [4], and about ten years later, Kolar et al. [5,6] reported the ternary phases $BaNd_2Ti_3O_{10}$ and $BaNd_2Ti_5O_{14}$. At almost the same time, Razogon et al. [7] reported the compound $BaNd_2Ti_4O_{12}$, and another compound, $Ba_{3.75}Pr_{9.5}Ti_{18}O_{54}$, was reported by Matveeva et al. [8]. Since then, several groups have investigated the microwave dielectric properties and the modification of ceramics in the $BaO–R_2O_3–TiO_2$ system [2,9–21], and many efforts also have been made to deal with the crystal-chemistry issues in the present system [10–14,16,17,19,20]. Now, the most acceptable formula for the solid solution phase with a TiO_2-rich composition in the $BaO–R_2O_3–TiO_2$ system is $Ba_{6-3x}R_{8+2x}Ti_{18}O_{54}$. However, both the higher and lower solid solution limits are still questionable. Ohsato et al. have systematically studied the $Ba_{6-3x}R_{8+2x}Ti_{18}O_{54}$ system, including the microwave dielectric properties and the crystal-chemistry issues. $Ba_{6-3x}R_{8+2x}Ti_{18}O_{54}$ have a tungsten bronze type structure composed of corner-sharing perovskite-like (TiO_6) octahedra. In the framework of linked octahedra, two pentagonal sites (A2) are occupied by Ba; five rhombic sites (A1) are occupied by Sm and Ba, with some vacancies; and the trigonal sites (C) are empty [9,10]. The extent of solubility x is reduced with decrease in the ionic radius of R ion [11,12]. For the largest La-containing analogue, the solid solution extends from $x = 0$ to 1, while for Nd and Sm analogues, several different range of x have been reported by different groups [9,13,14]. Ohsato et al. [13] determined the solid solution regions for the Nd and Sm systems: $0.0 \leq x \leq 0.7$ if R = Nd and $0.3 \leq x \leq 0.7$ if R = Sm. However, the recent work [14] modified the upper limit of x for $Ba_{6-3x}Nd_{8+2x}Ti_{18}O_{54}$ into 0.75, and it should also be an

* Corresponding author. Tel.: +86 571 87952112; fax: +86 571 87952112.
E-mail address: xmchen59@zju.edu.cn (X.M. Chen).

0272-8842/$36.00 © 2011 Published by Elsevier Ltd and Techna Group S.r.l.
doi:10.1016/j.ceramint.2011.06.012

interesting issue to determine the accurate solid solution limits for $Ba_{6-3x}Sm_{8+2x}Ti_{18}O_{54}$.

In the present work, $Ba_{6-3x}Sm_{8+2x}Ti_{18}O_{54}$ ceramics (x = 0.0, 1/10, 1/5, 1/4, 3/10, 1/2, 2/3, 7/10, 3/4, 4/5, 1.0) are prepared by a solid-state reaction method, and the lower and upper limits of x are determined by the means of Rietveld refinement of XRD data combined with the backscattered electron images. The variation tendency of microwave dielectric characteristics with compositions is also investigated for the present ceramics.

2. Experimental procedures

$Ba_{6-3x}Sm_{8+2x}Ti_{18}O_{54}$ (x = 0.0, 1/10, 1/5, 1/4, 3/10, 1/2, 2/3, 7/10, 3/4, 4/5, 1.0) ceramics were prepared by a solid-state reaction process where the reagent-grade $BaCO_3$ (99.93%), Sm_2O_3 (99.9%), TiO_2 (99.5%) powders were adopted as the raw materials. The weighed raw materials were mixed by ball milling with zirconia media in ethanol for 24 h, and then heated at 1250 °C in air for 3 h after drying. The calcined powders, with 7 wt% of PVA (polyvinyl alcohol) added, were pressed into the disks measuring 12 mm in diameter and 2–6 mm in thickness with a uniaxial pressure of 98 MPa, and then sintered at 1300–1400 °C in air for 3 h. After cooling from the sintering temperature to 1100 °C at a rate of 2 °C/min, the ceramics were naturally cooled inside the furnace.

The crystal phases of the sintered ceramics after crushing and grinding were determined by powder X-ray diffraction (XRD) analysis, using Cu Kα radiation (Rigaku D/max 2550PC, Rigaku Co., Tokyo, Japan). The backscattered electron micrographs of the polished and thermally etched surfaces of sintered disks were observed with a field emission scanning electron microscopy (SIRION, FEI, Netherlands). The XRD data for Rietveld analysis were collected over the range of 2θ = 10–130° with a step size of 0.02° and a count time of 2 s. The FULLPROF program was used for Rietveld structural refinement [22]. According to the program, in a mixture of N crystalline phases the weight fraction of W_j of phase j is given by:

$$W_j = \frac{S_j Z_j M_j V_j / t_j}{\sum_i [S_i Z_i M_i V_i / t_i} \qquad (1)$$

where S_j is the scale factor of the phase j, Z_j is the number of formula units per unit cell for phase j, M_j is the mass of the formula unit, V_j is the cell volume, and t_j is the Brindley particle absorption contrast factor for phase j.

The microwave dielectric constant ε_r and the temperature coefficient of resonant frequency τ_f were measured at 4.0–5.5 GHz by the Hakki–Coleman method [23], using a network analyzer (E8363B, Agilent Technologies, Palo Alto, CA). τ_f at microwave frequency was measured in the temperature range from 20 °C to 85 °C. The quality factor Q was evaluated around 5 GHz by the cavity reflection method [24], using a silver-coated cavity connected to the analyzer. Because Q factor is generally inversely proportional to the frequency f in the microwave region, Qf is commonly used to evaluate the dielectric loss instead of Q.

3. Results and discussion

Fig. 1 gives the XRD patterns of $Ba_{6-3x}Sm_{8+2x}Ti_{18}O_{54}$ dense ceramics with compositions of x = 0.0–1.0. The orthorhombic new tungsten bronze type structure in *Pbnm* space group (JCPD card No. 44-0062) is determined in the entire composition range. However, $BaTiO_3$ secondary phase is detected for x = 0.0, 1/10 and 1/5, and $Sm_2Ti_2O_7$ secondary phase is observed for x = 3/4, 4/5 and 1.0. It should be noted here that the solid solution regions for $Ba_{6-3x}Sm_{8+2x}Ti_{18}O_{54}$ was reported to be $0.3 \leq x \leq 0.7$ by Ohsato et al. [13]. Therefore, further investigation was carried out via Rietveld refinement analysis to confirm the accurate solubility limits.

The variation of lattice parameters a, b, c and V with x is shown in Fig. 2. In the range of $1/4 \leq x \leq 2/3$, the a, b, c and V values all decrease monotonically with the increase of x, and in the range of $0.0 \leq x \leq 1/4$ and $2/3 \leq x \leq 1.0$ there is a complex variation for these parameters. With increasing x, more substitution of $3Ba^{2+}$ by $2R^{3+}$ leads to the increase in the number of vacancies along with the decrease of volume of TiO_6 octahedra, and the increased number of vacancies together with the difference in ionic radii ($Ba^{2+} > 2R^{3+}$) result in the decrease of lattice parameters. The variation of lattice parameters a, b, c and V with x may indicate a different type of ion substitution for the four different sites of the crystal structure. That is, the non-monotonic variation of these parameters at x = 1/4 and x = 2/3 may give the evidence for the lower and upper limits of x in $Ba_{6-3x}Sm_{8+2x}Ti_{18}O_{54}$ solid solution.

Fig. 3 and Table 1 show the Rietveld analysis results of X-ray powder diffraction patterns of $Ba_{6-3x}Sm_{8+2x}Ti_{18}O_{54}$ with x = 1/5, x = 1/4, x = 2/3, x = 7/10 and x = 3/4. The XRD data are indexed as the orthorhombic $Ba_{6-3x}Sm_{8+2x}Ti_{18}O_{54}$ tungsten bronze single phase in the space group *Pbnm*, where a = 12.1836(4) Å, b = 22.3916(7) Å, c = 7.6865(2) Å and a = 12.1579(3) Å, b = 22.3038(5) Å, c = 7.6634(2) Å for x = 1/4 and x = 2/3, respectively. While, the situation for x = 1/5, x = 7/10 and

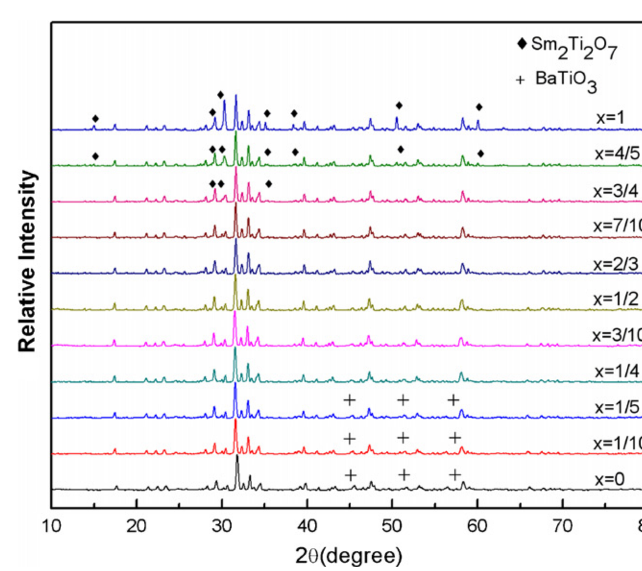

Fig. 1. XRD patterns of crashed powders of $Ba_{6-3x}Sm_{8+2x}Ti_{18}O_{54}$ ceramics in the range of $0 \leq x \leq 1$.

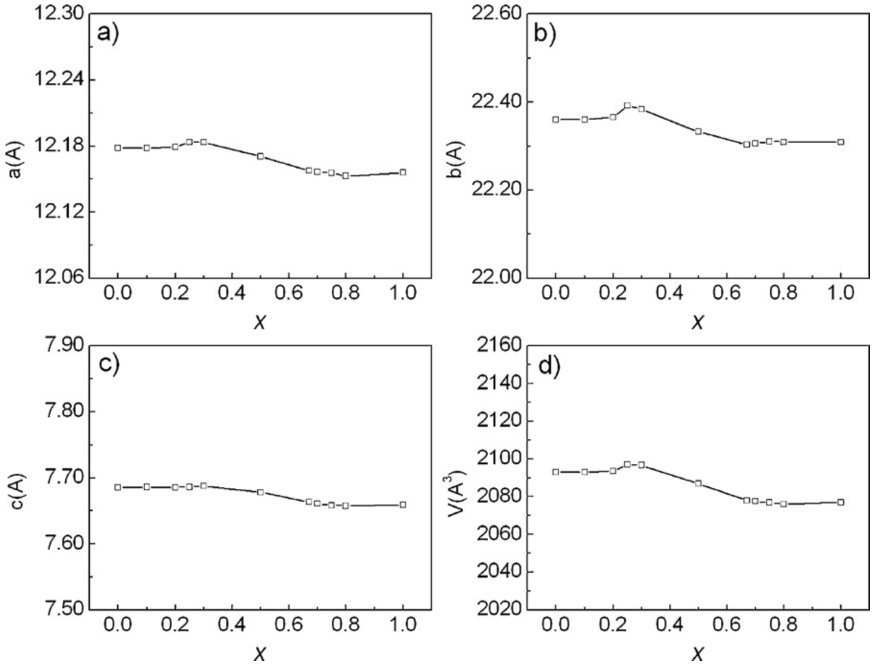

Fig. 2. Lattice parameters of $Ba_{6-3x}Sm_{8+2x}Ti_{18}O_{54}$ ceramics as function of x: (a) a, (b) b, (c) c, and (d) V.

$x = 3/4$ is very similar, but 4.71(15) wt% of $BaTiO_3$ secondary phase, 2.27(12) wt% of $BaTi_4O_9$ secondary phase and 3.40(9) wt% of $Sm_2Ti_2O_7$ secondary phase are detected, respectively.

Nearly full densification of $Ba_{6-3x}Sm_{8+2x}Ti_{18}O_{54}$ ceramics can be achieved at different temperatures for different compositions. The densification temperature is 1350 °C for the compositions $x = 0.0$, 1/10, and 1/5, a higher densification temperature of 1400 °C is observed for $x = 1/4$, 3/10, 1/2, and 7/10, and a relatively lower densification temperature of 1300 °C is observed for $x = 3/4$, 4/5 and 1.0, while the densification temperature for $x = 2/3$ is 1375 °C. There is a obvious tendency that a higher densification temperature is needed for the compositions with single phase structure, and the presence of secondary phase generally lowers the densification temperature due to the formation of liquid phase [25]. Pores are formed in the liquid phase, and the major change in free energy that takes place during densification is due to the decrease in surface area of pores in the liquid phase, and this provides the driving force for sintering to promote higher densification rates and lower the sintering temperatures [26,27]. And the only exceptions are $x = 2/3$ and 7/10 which need further investigation. The

Table 1
Experimental parameters for XRD of $Ba_{6-3x}Sm_{8+2x}Ti_{18}O_{54}$ for $x = 1/5$, 1/4, 2/3, 7/10 and 3/4.

	$x = 1/5$[a]	$x = 1/4$	$x = 2/3$	$x = 7/10$[b]	$x = 3/4$[c]
Unit cell (space group *Pbnm*)	$a = 12.1792(4)$ Å, $b = 22.3657(7)$ Å, $c = 7.6857(2)$ Å, $V = 2093.53(11)$ Å^3	$a = 12.1836(4)$ Å, $b = 22.3916(7)$ Å, $c = 7.6865(2)$ Å, $V = 2096.96(11)$ Å^3	$a = 12.1579(3)$ Å, $b = 22.3038(5)$ Å, $c = 7.6634(2)$ Å, $V = 2078.06(8)$ Å^3	$a = 12.1566(3)$ Å, $b = 22.3057(5)$ Å, $c = 7.6615(2)$ Å, $V = 2077.48(8)$Å^3	$a = 12.1557(3)$ Å, $b = 22.3107(6)$ Å, $c = 7.6584(2)$ Å, $V = 2076.95(9)$ Å^3
Number of reflections	4048	4038	3969	3816	3971
Number of refined	116	103	107	116	121
Half width parameters	$U = 0.223(9)$, $V = -0.081(6)$, $W = 0.031(1)$	$U = 0.232(9)$, $V = -0.111(6)$, $W = 0.034(1)$	$U = 0.173(6)$, $V = -0.090(4)$, $W = 0.032(1)$	$U = 0.165(6)$, $V = -0.087(4)$, $W = 0.031(1)$	$U = 0.164(6)$, $V = -0.088(5)$, $W = 0.032(1)$
Peak shape, η	Pseudo-Voigt, 0.718(23)	Pseudo-Voigt, 0.720(21)	Pseudo-Voigt, 0.670(17)	Pseudo-Voigt, 0.672(18)	Pseudo-Voigt, 0.593(18)
Zero point, 2θ (°)	−0.0026(16)	−0.0257(15)	0.0312(11)	−0.0167(11)	−0.0289(12)
Asymmetry parameter	$P1 = 0.080(4)$, $P2 = 0.033(1)$	$P1 = 0.091(4)$, $P2 = 0.033(1)$	$P1 = 0.125(3)$, $P2 = 0.036(1)$	$P1 = 0.133(3)$, $P2 = 0.042(1)$	$P1 = 0.112(4)$, $P2 = 0.038(1)$
Reliability factors	$R_p = 4.31$, $R_{wp} = 5.70$, $\chi^2 = 1.36$	$R_p = 4.99$, $R_{wp} = 6.63$, $\chi^2 = 2.12$	$R_p = 4.35$, $R_{wp} = 5.78$, $\chi^2 = 1.54$	$R_p = 4.52$, $R_{wp} = 6.01$, $\chi^2 = 1.86$	$R_p = 4.48$, $R_{wp} = 5.91$, $\chi^2 = 1.46$

[a] 4.71(15) wt% secondary phase of $BaTiO_3$ (*P4/mmm*, $a = 3.9970(2)$ Å, $b = 3.9970(2)$ Å and $c = 4.0237(4)$ Å) is detected.
[b] 2.27(12) wt% secondary phase of $BaTi_4O_9$ (*Pmmn*, $a = 14.4375(44)$ Å, $b = 3.7807(8)$ Å and $c = 6.2279(19)$ Å) is detected.
[c] 3.40(9) wt% secondary phase of $Sm_2Ti_2O_7$ (*Fd−3m*, $a = 10.2102(3)$ Å, $b = 10.2102(3)$ Å and $c = 10.2102(3)$ Å) is detected.

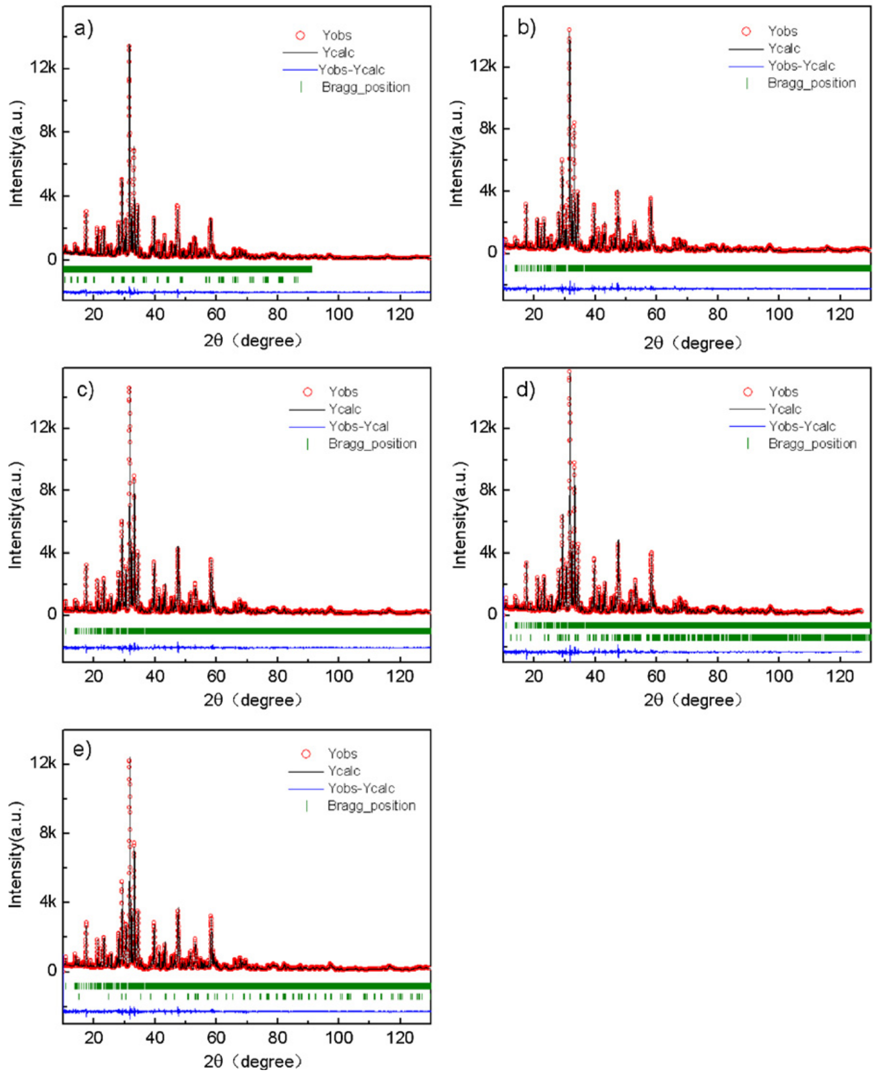

Fig. 3. Rietveld analysis results of XRD patterns for $Ba_{6-3x}Sm_{8+2x}Ti_{18}O_{54}$ powders: (a) $x = 1/5$, (b) $x = 1/4$, (c) $x = 2/3$, (d) $x = 7/10$, (e) $x = 3/4$; experimental, calculated and difference. 4.71(15) wt% secondary phase of $BaTiO_3$ (*P*4/*mmm*, $a = 3.9970(2)$ Å, $b = 3.9970(2)$ Å and $c = 4.0237(4)$ Å) is detected for $x = 1/5$; and 2.27(12) wt% secondary phase of $BaTi_4O_9$ (*Pmmn*, $a = 14.4375(44)$ Å, $b = 3.7807(8)$ Å and $c = 6.2279(19)$ Å) is detected of $x = 7/10$; 3.40(9) wt% secondary phase of $Sm_2Ti_2O_7$ (*Fd*−3*m*, $a = 10.2102(3)$ Å, $b = 10.2102(3)$ Å and $c = 10.2102(3)$ Å) is detected for $x = 3/4$.

backscattered electron images of thermally etched surfaces of $Ba_{6-3x}Sm_{8+2x}Ti_{18}O_{54}$ ceramics are shown in Fig. 4. Since the lattice parameter in *c*-axis is much smaller than those in *a*- and *b*-axis, and the growth rate of crystal is faster for the *c*-axis direction than that for the *a*- and *b*-axis [28], $Ba_{6-3x}R_{8+2x}Ti_{18}O_{54}$ ceramics tend to indicate columnar grain morphology. The obvious columnar grain morphology is observed for the present ceramics with $x \leq 2/3$, while the equiaxed grain morphology is observed for $x > 2/3$. This is because the compositions of $x \geq 3/4$ are sintered at a lower sintering temperature of 1300 °C, while a higher temperature is needed to form the columnar grain morphology for the present ceramics.

The microwave dielectric characteristics of $Ba_{6-3x}Sm_{8+2x}Ti_{18}O_{54}$ ceramics are shown in Fig. 5 as the functions of composition *x*. The dielectric constant decreases monotonically with increasing *x*, from 93 to 77. *Qf* value increases at first, reaches the maximum around $x = 2/3$, and turns to decrease for $x > 7/10$. There is a complex variation tendency of τ_f, and the small τ_f is observed for the compositions $1/2 \leq x \leq 4/5$. In the compositions $0 \leq x \leq 1/5$, no resonant peak can be observed in the microwave region. The best microwave dielectric properties obtained are: $\varepsilon_r = 82.7$, $Qf = 10{,}025$ GHz, $\tau_f = -9.2$ ppm/°C for $x = 2/3$ in which *R* and Ba ions separately occupy the rhombic sites (A1) and the pentagonal sites (A2); and $\varepsilon_r = 80.8$, $Qf = 10{,}000$ GHz, $\tau_f = -12.8$ ppm/ °C for $x = 7/10$ in which there is a small amount of $BaTi_4O_9$ secondary phase.

The high *Qf* value at $x = 2/3$ can be interpreted by the lowest crystal distortion inner stress as a result of the ordering of *R* and Ba ions in the A1 and A2 sites, respectively. As *x* increases in the range of $0 \leq x \leq 2/3$, Ba ions with larger ionic radii will occupy also a part of the rhombic sites (A1) with their smaller size and the number of Ba in A1 sites reduces. The occupation of Ba ions in A1 site leads to the internal strain around themselves which lowers the *Qf* value. Moreover, the vacancies

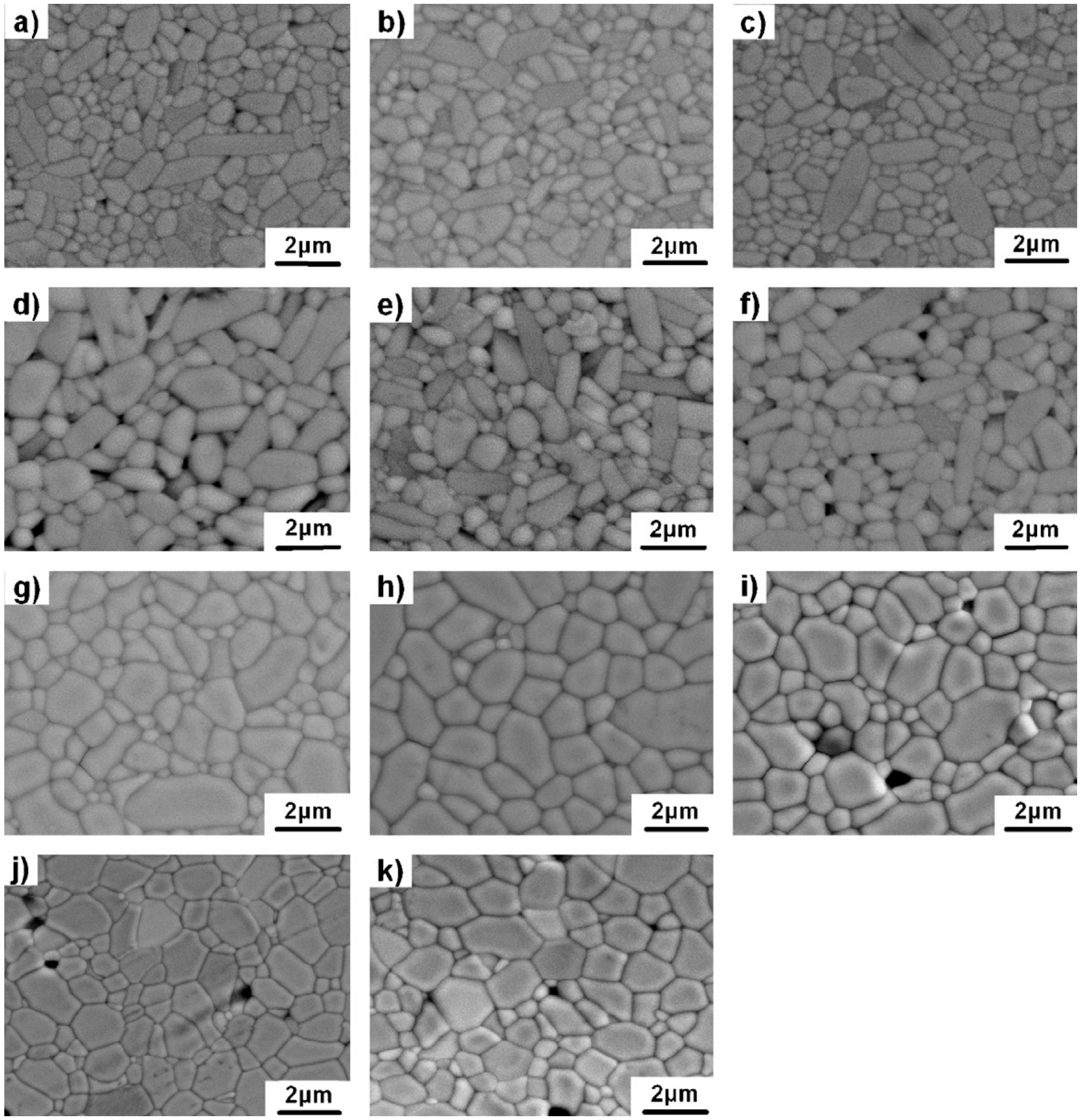

Fig. 4. Backscattered electron images of thermally etched surfaces of $Ba_{6-3x}Sm_{8+2x}Ti_{18}O_{54}$ dense ceramics with various compositions. (a) $x = 0.0$ sintered at 1350 °C, (b) $x = 1/10$ sintered at 1350 °C, (c) $x = 1/5$ sintered at 1350 °C, (d) $x = 1/4$ sintered at 1400 °C, (e) $x = 3/10$ sintered at 1400 °C, (f) $x = 1/2$ sintered at 1400 °C, (g) $x = 2/3$ sintered at 1375 °C, (h) $x = 7/10$ sintered at 1400 °C, (i) $x = 3/4$ sintered at 1300 °C, (j) $x = 4/5$ sintered at 1300 °C, and (k) $x = 1.0$ sintered at 1300 °C.

generated in A1 sites by the substitution of $3Ba^{2+}$ by $2R^{3+}$ with increasing x might be the second reason for lowering the internal strain and lead to the high Qf value, and the amount of vacancies is proportional to the x value. On the other hand, as x increases in the range of $2/3 \leq x \leq 1$, Ba ions in A2 sites are substituted partly by R ions. The decrease of Ba ions produces vacancies in A2 sites and may lead to unstable crystal structure, and the decrease in the number of vacancies in A1 sites combined with the decrease of Ba ions in the A2 sites might lead to the additional internal strain. These strains are the reasons for the lower quality factor at the $2/3 \leq x \leq 1$. The high Qf value (>10,000 GHz) at $x = 7/10$ which exceeds the upper limit of x is much higher than those reported previously [9]. The possible reason for the high Qf value in $x = 7/10$ is the release of inner stress due to the separation of the secondary phase from the solid solution.

The Clausius–Mosotti equation shows explicitly how dielectric constant depends on composition and crystal structure through polarizability and molar volume as following:

$$\varepsilon' = \frac{3V_m + 8\pi\alpha_D^T}{3V_m - 4\pi\alpha_D^T} \quad (2)$$

where V_m is the cell volume, and α_D^T is the total dielectric polarizability. As investigated by Shannon [29], the polarizability of Sm^{3+} (4.74 Å^3) is considerably lower than that of Ba^{2+} (6.40 Å^3) and consequently the total polarizabilities re-

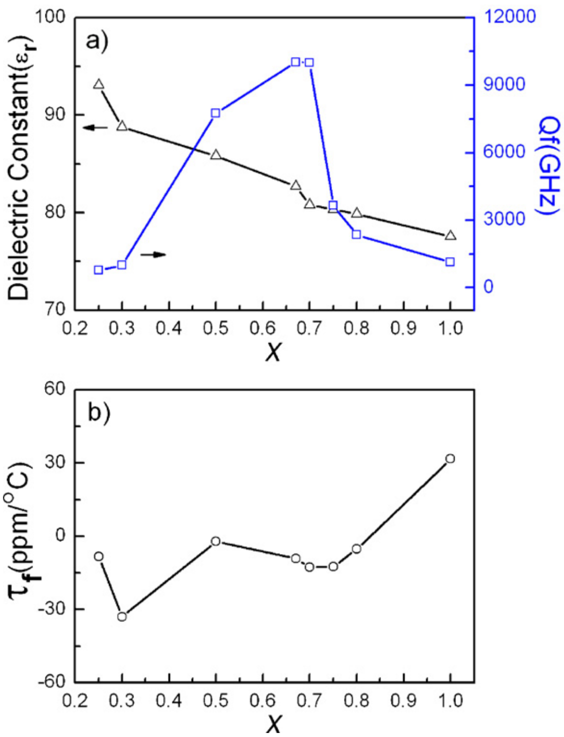

Fig. 5. Microwave dielectric characteristics of $Ba_{6-3x}Sm_{8+2x}Ti_{18}O_{54}$ ceramics as functions of composition x: (a) ε_r and Qf value as functions of x and (b) τ_f as functions of x.

duced significantly with increasing x (from 3×6.40 to 2×4.74 Å^3 due to the substitution of Sm^{3+} for Ba^{2+}), which leads to the decrease of ε_r. On the other hand, the decrease of V_m results in the increase of ε_r, but it is relatively not so much. Therefore, there is a decrease of ε_r with x. Meanwhile, other effects should also be considered, such as tilting of the TiO_6 octahedra strings [15]. The τ_f value of the present system is negative and close to zero in the whole range as those reported previously, except that a lower τ_f (-33.0 ppm/°C) value is indicated for $x = 3/10$ and a relatively large and positive τ_f (31.6 ppm/°C) value for $x = 1.0$, which disagrees with the data reported by Ohsato et al. [19]. Moreover, the τ_f value increases almost linearly and changes from negative to positive in the region of $3/4 \leq x \leq 1.0$, which results possibly from the increasing amount of $Sm_2Ti_2O_7$ secondary phase which has a high τ_f (about 248.8 ppm/°C calculated from the data by Takahashi [30]).

4. Conclusions

The upper solubility limit for $Ba_{6-3x}Sm_{8+2x}Ti_{18}O_{54}$ tungsten bronze ceramics is $x = 2/3$, while the lower solubility limit is 1/4 instead of the previously reported one $x = 3/10$. The dielectric constant of $Ba_{6-3x}Sm_{8+2x}Ti_{18}O_{54}$ ceramics decreases monotonically with increasing x, while the small temperature coefficient of resonant frequency with complex variation tendency is observed for the compositions $1/2 \leq x \leq 4/5$. The Qf value increases at first, reaches the maximum around $x = 2/3$, and turns to decrease for $x > 7/10$. The best microwave dielectric properties obtained are: $\varepsilon_r = 82.7$, $Qf = 10{,}025$ GHz, $\tau_f = -9.2$ ppm/°C for $x = 2/3$ and $\varepsilon_r = 80.8$, $Qf = 10{,}000$ GHz, $\tau_f = -12.8$ ppm/°C for $x = 7/10$.

Acknowledgement

The present work was supported by Chinese National Basic Research Program under grant number 2009CB623302.

References

[1] T.A. Vanderah, Talking ceramics, Science 298 (2002) 1182–1184.
[2] I.M. Reaney, D. Iddles, Microwave dielectric ceramics for resonators and filters in mobile phone networks, J. Am. Ceram. Soc. 89 (2006) 2063–2072.
[3] X.M. Chen, Y. Li, A- and B site cosubstituted $Ba_{6-3x}Sm_{8+2x}Ti_{18}O_{54}$ microwave dielectric ceramics, J. Am. Ceram. Soc. 85 (2002) 579–584.
[4] R.L. Bolton, Temperature Compensating Ceramics Capacitors in the System Baria–Rare-earth-oxide Titania, PhD Thesis, Ceramic Engineering, University of Illinois, Urbana, IL, 1968.
[5] D. Kolar, Z. Stadler, S. Gaberscek, D. Suvorov, Ceramic and dielectric properties of selected compositions in the $BaO–TiO_2–Nd_2O_3$ system, Ber. Dt. Keram. Ges. 55 (1978) 346–347.
[6] D. Kolar, Z. Stadler, S. Gaberscek, H.S. Parker, R.S. Roth, Synthesis and crystal chemistry of $BaNd_2Ti_3O_{10}$, $BaNd_2Ti_5O_{14}$, and $Nd_4Ti_9O_{24}$, J. Solid State Chem. 38 (1981) 158–164.
[7] E.S. Razogon, A.M. Gens, M.B. Varfolomeev, S.S. Korovin, V.S. Kostomarov, The complex barium and lanthanum titanates, Russ. J. Inorg. Chem. 25 (6) (1980) 945–947.
[8] R.G. Matveeva, M.B. Varfolomeev, L.S. Il'yuschenko, Refinement of the composition and crystal structure of $Ba_{3.75}Pr_{9.5}Ti_{18}O_{54}$, Russ. J. Inorg. Chem. 29 (1) (1984) 31–34 (in Russian).
[9] T. Negas, P.K. Davies, Influence of chemistry and processing on the electrical properties of $Ba_{6-3x}Ln_{8+2x}Ti_{18}O_{54}$ solid solutions, in: T. Negas, H. Ling (Eds.), Materials and Processes for Wireless Communication, Ceram. Trans., vol. 53, The American Ceramic Society, Westerville, OH, 1995, pp. 179–196.
[10] H. Ohsato, Science of tungsten bronze-type like $Ba_{6-3x}R_{8+2x}Ti_{18}O_{54}$ (R = rare earth) microwave dielectric solid solutions, J. Eur. Ceram. Soc. 21 (2001) 2703–2711.
[11] R. Ubic, I.M. Reaney, W.E. Lee, Microwave dielectric solid-solution phase in system $BaO–Ln_2O_3–TiO_2$ (Ln = lanthanide cation), Int. Mater. Rev. 43 (5) (1998) 205–219.
[12] K.M. Cruickshank, X.P. Jing, G. Wood, E.E. Lachowski, A.R. West, Barium neodymium titanate electroceramics: phase equilibria studies of $Ba_{6-3x}Nd_{8+2x}Ti_{18}O_{54}$ solid solution, J. Am. Ceram. Soc. 76 (1996) 1605–1610.
[13] H. Ohsato, T. Ohhashi, S. Nishigaki, T. Okuda, K. Sumiya, S. Suzuki, Formation of solid solution of new tungsten bronze-type microwave dielectric compounds $Ba_{6-3x}R_{8+2x}Ti_{18}O_{54}$ (R = Nd and Sm $0 \leq x \leq 1$), Jpn. J. Appl. Phys. 32 (1993) 4323–4326.
[14] L. Zhang, X.M. Chen, N. Qin, X.Q. Liu, Upper limit of x in $Ba_{6-3x}Nd_{8+2x}Ti_{18}O_{54}$ new tungsten bronze solid solution, J. Eur. Ceram. Soc. 27 (2007) 3011–3016.
[15] M. Valant, D. Suvorov, C.J. Rawn, Intrinsic reasons for variations in dielectric properties of $Ba_{6-3x}R_{8+2x}Ti_{18}O_{54}$ (R = La–Gd) solid solutions, Jpn. J. Appl. Phys. 38 (1999) 2820–2826.
[16] A.M. Gens, M.B. Varfolomeev, V.S. Kostomarov, S.S. Korovin, Crystal-chemical and electrophysical properties of complex titanates of barium and lanthanides, Russ. J. Inorg. Chem. 26 (1981) 482–484.
[17] M. Valant, D. Suvorov, D. Kolar, X-ray investigations and determination of the dielectric properties of the compound $Ba_{4.5}Gd_9Ti_{18}O_{54}$, Jpn. J. Appl. Phys. 35 (1996) 144–150.
[18] P. Laffez, G. Desgardin, B. Raveau, Influence of calcination, sintering and composition upon microwave properties of the $Ba_{6-x}Sm_{8+2x/3}Ti_{18}O_{54}$-type oxide, J. Mater. Sci. 27 (1992) 5229–5238.
[19] H. Ohsato, T. Ohhashi, H. Kato, S. Nishigaki, T. Okuda, Microwave dielectric properties and structure of the $Ba_{6-3x}Sm_{8+2x}Ti_{18}O_{54}$ solid solution, Jpn. J. Appl. Phys. 34 (1995) 187–191.

[20] H. Ohsato, Y. Futamata, H. Sakashita, N. Araki, K. Kakimoto, S. Nishigaki, Configuration and coordination number of cation polyhedra of tungsten bronze-type-like $Ba_{6-3x}Sm_{8+2x}Ti_{18}O_{54}$ solid solutions, J. Eur. Ceram. Soc. 23 (2003) 2529–2533.
[21] H. Ohsato, Research and development of microwave dielectric ceramics for wireless communications, J. Ceram. Soc. Jpn. 113 (2005) 703–711.
[22] J. Rodriguez-Carvajal, Recent developments of the program FULLPROF, Int. Union Crystallogr. Newsl. 26 (2001) 12–19.
[23] W. Hakki, P.D. Coleman, A dielectric resonant method of measuring inductive capacitance in the millimeter range, IRE Trans. Microwave Theory Tech. 8 (1960) 402–410.
[24] X.C. Fan, X.M. Chen, X.Q. Liu, Complex permittivity measurement on high Q materials via combined numerical approaches, IEEE Trans. Microwave Theory Tech. 53 (10) (2005) 3130–3134.
[25] Y. Ota, K. Kakimoto, H. Ohsato, S. Nishigaki, Low-temperature sintering and microwave dielectric property of $Ba_{6-3x}Sm_{8+2x}Ti_{18}O_{54}$ solid solution, J. Ceram. Soc. Jpn. 110 (2002) 108–114 (in Japanese).
[26] W.D. Kingery, Densification during sintering in the presence of a liquid phase. I. Theory, J. Appl. Phys. 30 (3) (1959) 301–306.
[27] R. Tandon, J. Johnson, Liquid-phase sintering, ASM Handbook, Powder Metal Technologies and Applications, vol. 7, 1998, pp. 565–573.
[28] K. Wada, K. Kakimoto, H. Ohsato, Microstructure and microwave dielectric properties of $Ba_4Sm_{9.33}Ti_{18}O_{54}$ ceramics containing columnar crystals, J. Eur. Ceram. Soc. 23 (2003) 2535–2539.
[29] R.D. Shannon, Dielectric polarizabilities of ions in oxides and fluorides, J. Appl. Phys. 73 (1) (1993) 348–366.
[30] J. Takahashi, K. Kageyama, T. Hayashi, Dielectric properties of double-oxide ceramics in the system Ln_2O_3–TiO_2 (Ln = La, Nd, Sm), Jpn. J. Appl. Phys. 30 (1991) 2354–2358.